Data reconciliation of an open channel flow network using modal decomposition

Qingfang Wu [a,*], Xavier Litrico [b], Alexandre M. Bayen [a]

[a] Department of Civil and Environmental Engineering, UC Berkeley, CA, USA
[b] Cemagref, UMR G-EAU, B.P. 5095, 34196 Montpellier Cedex 5, France

ARTICLE INFO

ABSTRACT

This article presents a method to estimate flow variables for an open channel network governed by the linearized Saint-Venant equations and subject to periodic forcing. The discharge at the upstream end of the system and the stage at the downstream end of the system are defined as the model inputs; the flow properties at selected internal locations, as well as the other external boundary conditions, are defined as the outputs. Both inputs and outputs are affected by noise and we use the model to improve the data quality. A spatially dependent transfer matrix in the frequency domain is constructed to relate the model input and output using modal decomposition. A data reconciliation technique is used to incorporate the error in the measured data and results in a set of reconciliated external boundary conditions; subsequently, the flow properties at any location in the system can be accurately estimated from the input measurements. The applicability and effectiveness of the method is demonstrated with a case study of the river flow subject to tidal forcing in the Sacramento-San Joaquin Delta, in California. We used existing USGS sensors in place in the Delta as measurement points, and deployed our own sensors at selected locations to produce data used for the validation. The proposed method gives an accurate estimation of the flow properties at intermediate locations within the channel network.

© 2008 Elsevier Ltd. All rights reserved.

1. Introduction

In hydraulic systems, numerous factors could lead to measurement errors, for example broken gauges, process leaks, sensor drifts, improper use of measuring devices and other random sources [1]. Data reconciliation, is an effective method to tune-up the measurement data [21,5,10,2], which has been applied in several engineering fields [11,3,20,25]. The objective of data reconciliation is to use information redundancy to handle errors in real-time measurements.

In the field of process control, data reconciliation is a part of the general state estimation or reconstruction process for dynamical systems, using Kalman filtering [8]. However, in certain cases, and for given time intervals, dynamic effects can sometimes be neglected which leads to simplified versions of the general approach, applicable to static models.

This article presents theoretical results applicable to data reconciliation for tidally forced networks of open channels. Using modal decomposition techniques, we are able to transform dynamic constraints into static constraints in the frequency domain, and subsequently obtain a static data reconciliation problem, which is easier to resolve and can lead to accurate results. Generally, this static data reconciliation problem is to minimize the measurement errors while satisfying the static constraints of the proposed model.

The proposed linear network model is constructed on the basis of analytical solutions to the *Linearized Saint-Venant equations* (LSVE) in the frequency domain [9,12,4]. With the assumption of a backwater curve model [22], a more realistic transfer matrix function has been introduced [16], which we use in the present article.

This article extends the general transfer matrix function approach to a channel network. A spatially dependent transfer matrix is constructed, relating a selected set of model inputs to the output variables. The transfer matrix is a function of channel width, channel length, bed slope, mean discharge, mean stage and Manning coefficient. This set of parameters needs to be chosen carefully to characterize the geometry of the channels, as the uncertainty of the parameters would contribute to the errors in the model output.

With this linear model in the frequency domain, the static data reconciliation problem is shown to be equivalent to a quadratic problem. The objective function used in the present study is a weighted L_2-norm of the difference between the measured and reconciliated data. The linear network model constructed serves as the constraints in the optimization problem. A closed-form optimal solution is obtained, resulting in a set of reconciliated boundary data consistent with both the linear network model and the

* Corresponding author. Tel.: +1 510 642 9569.
E-mail addresses: qingfangwu@berkeley.edu (Q. Wu), xavier.litrico@cemagref.fr (X. Litrico), bayen@berkeley.edu (A.M. Bayen).

statistical assumptions on measurement errors. Subsequently, we apply the reconstructed boundary conditions to the linear network model to obtain an accurate forward simulation of the flow within of the network domain.

This article is organized as follows: Section 2 introduces the general framework of linear models, i.e., LSVE in the frequency domain, the spatially dependent transfer matrix. A channel network model featuring one-dimensional non-uniform flow is subsequently described, and the solution of the data reconciliation problem in the static case is addressed. Section 3 applies the linear model to a channel network in the Sacramento-San Joaquin Delta in California. Static data reconciliation is applied to handle the errors in the measurements. The effectiveness of the method is assessed by correlating the model estimations with field data at three intermediate locations in the network, which serve as validation points. Section 4 summarizes the study and presents the scope of our future work.

2. Proposed method

2.1. General considerations

The general class of hydraulic system studied in the present article is a distributed network of channels subject to quasi-periodic tidal forcing. Sensing on this hydraulic system is done using fixed Eulerian *US Geological Survey* (USGS) sensors, subject to measurement errors. The motivation of the work is to derive the "most likely" flow conditions from the measured data available in a given period of time (at least a few weeks to catch the tidal period), and forecast the future flow variables. The goal of the method is thus not real time estimation, as traditionally done in data assimilation [23], but forecast based on measured forcing.

The flow variables are related to each other by a mathematical model. Therefore, if the measurement data was error free, it would satisfy the model. Because the number of points at which the variables are measured is usually larger than needed to fully prescribe the model, there is "information redundancy" in the system. Once information redundancy exists, data reconciliation can be implemented to account for measurement error.

The ultimate goal of data reconciliation is to use such information redundancy in a system to have the data self-corrected using the model. An effective data reconciliation method allows the detection of any inconsistent or biased measurements, and furthermore provides corrected values (namely estimated measurements).

It should be noted that any information redundancy is model-specific. We therefore need to first construct a "good" hydraulic model to characterize the flow system, as described in the following section.

2.2. Linear channel network model

2.2.1. Transfer matrix representation of Saint-Venant model

The *Linearized Saint-Venant Equations* (LSVE) have been widely used in the open-channel hydraulic systems literature [7,15,17,14]. They describe the perturbed discharge $q(x,t)$ and stage $y(x,t)$ with two coupled *partial differential equations* (PDEs). For a rectangular cross-section, these equations are given by

$$T_0 \frac{\partial y}{\partial t} + \frac{\partial q}{\partial x} = 0 \tag{1}$$

$$\frac{\partial q}{\partial t} + 2V_0(x)\frac{\partial q}{\partial x} - \beta_0(x)q + \alpha_0(x)\frac{\partial y}{\partial x} - \gamma_0(x)y = 0 \tag{2}$$

where $\alpha_0(x)$, $\beta_0(x)$ and $\gamma_0(x)$ are given by

$$\alpha_0 = (C_0^2 - V_0^2)T_0 \tag{3}$$

$$\beta_0 = -\frac{2g}{V_0}\left(S_b - \frac{dY_0}{dx}\right) \tag{4}$$

$$\gamma_0 = gT_0\left[(1+\kappa_0)S_b - (1+\kappa_0 - (\kappa_0 - 2)F_0^2)\frac{dY_0}{dx}\right] \tag{5}$$

with $\kappa_0 = 7/3 - 8Y_0/(3(2Y_0 + T))$; T_0 is denoted as a uniform width at the free surface, $C_0 = \sqrt{gY_0}$ is the wave celerity, $F_0 = V_0/C_0$ is the Froude number, $V_0 = Q_0/A_0$ is the steady state velocity, Q_0 is the average discharge along the channel and $Y_0(X)$ is the average stage at the downstream point of the channel, X is the river reach length (m), S_b is the bed slope (m/km).

The upstream and downstream boundary conditions are the upstream discharge perturbation $q(0,t)$ and the downstream stage perturbation $y(X,t)$, respectively. The initial conditions are given by $y(x,0) = 0$ and $q(x,0) = 0$ for all $x \in [0,X]$.

To facilitate the mathematical analysis, we rewrite the linearized Saint-Venant equations as follows:

$$\frac{\partial}{\partial t}\begin{pmatrix} q(x,t) \\ y(x,t) \end{pmatrix} = \left(\mathscr{A}(x)\frac{\partial}{\partial x} + \mathscr{B}(x)\right)\begin{pmatrix} q(x,t) \\ y(x,t) \end{pmatrix} \quad (x,t) \in [0,X] \times [0,+\infty) \tag{6}$$

where

$$\mathscr{A}(x) = \begin{pmatrix} -2V_0 & -\alpha_0 \\ -\frac{1}{T_0} & 0 \end{pmatrix}, \quad \mathscr{B}(x) = \begin{pmatrix} \beta_0 & \gamma_0 \\ 0 & 0 \end{pmatrix} \tag{7}$$

The application of Laplace transform to the linear PDE system (6) leads to the following *ordinary differential equations* (ODEs) in the variable x, with a complex parameter s:

$$\frac{d}{dx}\begin{pmatrix} q(x,s) \\ y(x,s) \end{pmatrix} = \mathscr{A}^{-1}(x)[\mathscr{B}(x) - s\mathbb{I}_2]\begin{pmatrix} q(x,s) \\ y(x,s) \end{pmatrix} \tag{8}$$

Following the method developed in [22], and further modified in [16], a transfer matrix $\mathscr{G}(x,X,s) = (g_{ij}(x,X,s))$ for the non-uniform channel relates the boundary conditions and intermediate flow variables, and is defined by the following equation

$$\begin{pmatrix} q(x,s) \\ y(x,s) \end{pmatrix} = \mathscr{G}(x,X,s)\begin{pmatrix} q(0,s) \\ y(X,s) \end{pmatrix} \tag{9}$$

$\mathscr{G}(x,X,s)$ is a function of channel length X, average discharge Q_0, average downstream depth Y_X, average width T_0, bed slope S_b and Manning coefficient n of the channel. The upstream and downstream boundary conditions are the upstream discharge perturbation $q(0,s)$ and the downstream stage perturbation $y(X,s)$, respectively. Because of the distributed nature of the system, this transfer function also depends on the coordinate x in the channel, since it relates inputs $q(0,s)$ and $y(X,s)$ to the state of the system $q(x,s)$ and $y(x,s)$ at any x in the channel. Please refer to the appendix for the details about the transfer matrix.

2.2.2. Transfer matrix model for channel networks

The model (9) can be readily applied to tidally driven channel networks. The problem of interest can be stated as follows, and is illustrated in Fig. 1. Given a set of "external" boundary conditions of a network, at which we have measurements, reconstruct flow conditions at "internal" locations (also referred to as boundary conditions). This type of problem appears in our data assimilation work, in which we need estimates of boundary conditions at locations where fixed sensors are not available. The fundamental approach to build a network model is as follows:

- *Step 1:* Decompose the channel network into individual channel reaches, and apply the linear model (9) to each branch. For each of the river reach indexed by i, the flow variables $q_i(x,s)$, $y_i(x,s)$
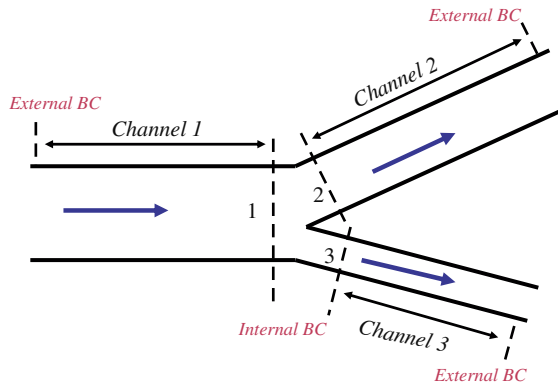
Fig. 1. Representation the system of interest for estimating internal boundary conditions (Internal BC) using data reconciliation on external boundary conditions (External BC): data is given at the three external conditions of channel 1–3; the state of the system is computed at three internal locations of the system labeled 1–3.

denote the perturbed discharge and stage in the frequency domain, respectively, X_i denote the length of the channel. The junction of the river reach is defined as the node of the channel network.

- *Step 2:* Impose the internal boundary conditions at every junction to ensure flow compatibility. Considering a simple river junction illustrated in Fig. 1: for each channel i, we will have the upstream boundary condition $y_i(0, s)$, $q_i(0, s)$, and downstream boundary condition $y_i(X_i, s)$, $q_i(X_i, s)$. If these boundary conditions are at the inside nodes of the channel network, they are called internal boundary conditions, otherwise they are labeled as external boundary conditions. The linear relationships of hydraulic internal boundary conditions at a junction are specified by equations of mass and energy conservation. Assuming no change in storage volume within the junction, the continuity equation can be expressed by

$$q_1(X_1, s) = q_2(0, s) + q_3(0, s)$$

When the flows in all the branches meeting at a junction are subcritical, the equation for energy conservation can be approximated by a kinematic compatibility condition as

$$y_1(X_1, s) = y_2(0, s) = y_3(0, s)$$

where X_i is the downstream point of each channel i, and 0 is the upstream point of each channel i.

- *Step 3:* Assemble the equations for each individual channel and interior junctions together to model the entire network. The flow variables at the boundary of each channel are represented by a linear relationship:

$$M(s)Z(s) = 0 \qquad (10)$$

where $Z(s)$ is the concatenated vector of all $[q_i(0, s), q_i(X_i, s), y_i(0, s), y_i(X_i, s)]^T$, $i = 1, \ldots, N$, $Z(s)$ is thus the vector comprising the discharge and stage variables at the upstream and downstream ends of all channels; $M(s)$ is a matrix of appropriate dimension encoding the previous constraints.

- *Step 4:* Evaluate the unmeasured flow variables inside the channel network:
  - (a) Specify the interior boundaries. In a channel network system, we define a subjective subset of boundary conditions ($Z_{given\,BC} \subset Z$), which leads to a unique solution of model (10). This subset should satisfy: $\dim(Z_{given\,BC}) = \dim(Z) - \text{Rank}(M)$. All the other unknown boundary variables (interior and external), denoted as $Z_{other\,BC} = Z \setminus Z_{given\,BC}$, are therefore estimated with model (10). Model (10) now has the form:

$$Z_{other\,BC} = R(s)Z_{given\,BC} \qquad (11)$$

where $R(s)$ is a matrix of appropriate size. Given $Z = \begin{pmatrix} Z_{given\,BC} \\ Z_{other\,BC} \end{pmatrix}$, $M(s) = [R(s)| - \mathbb{I}]$.

  - (b) Estimation of the perturbed discharge and stage along the channel. It is achieved by a simple application of transfer function analysis:

$$\begin{pmatrix} q_i(x, s) \\ y_i(x, s) \end{pmatrix} = \begin{pmatrix} g_{i,11}(x, X_i, s) & g_{i,12}(x, X_i, s) \\ g_{i,21}(x, X_i, s) & g_{i,22}(x, X_i, s) \end{pmatrix} \begin{pmatrix} q_i(0, s) \\ y_i(X_i, s) \end{pmatrix},$$
$$i = 1, \ldots, N \qquad (12)$$

where $\mathscr{G}_i(x, X_i, s) = (g_{i,jk}(x, X_i, s))$ is the distributed transfer matrix based on the information of channel i.

2.3. Data reconciliation

In practice, the measured data called Y_m is normally a superset of the data required to uniquely define the system. i.e., $Z_{given\,BC} \subset Y_m \subseteq Z$. When this is the case, we can use the information redundancy and apply data reconciliation to detect and handle the measurement errors. Data reconciliation requires a process model and statistical characteristics of the measurements.

Using modal decomposition, we are able to convert the dynamic model (6) to a "static" model, in which the measurable variables are linked by an algebraic relationship in the frequency domain:

$$P(s)Y(s) = 0 \qquad (13)$$

where $Y(s) = [Y_1, Y_2, Y_3, \ldots] \subseteq Z(s)$ is a vector of noise free measurements, and $P(s)$ is a sub-matrix of $M(s)$ with the appropriate dimension.

It is assumed that the measurements are independent and subject to an additive noise. The measured data Y_m is composed of the "ideal" measurements vector Y and a noise vector ϵ:

$$Y_m = Y + \epsilon \qquad (14)$$

This noise vector ϵ is assumed to follow a Gaussian distribution with zero mean and *weight matrix* $W = \text{diag}(\sigma_1^2, \sigma_2^2, \ldots, \sigma_n^2)$. Here σ_i represents the noise standard deviation for each measurement. Note that the matrix W is chosen (positive definite), and that its components are picked to minimize the error, in the present case a weighted L^2 norm.

The objective of data reconciliation is to obtain estimated values $\widehat{Y}$ close to the measurements Y_m while satisfying the "static" linear model (13). This can be formulated as an optimization problem with linear constraints. The cost function to minimize is the weighted quadratic error between the measurements Y_m and the reconciliated data $\widehat{Y}$. The constraints are given by the model (13). The reconciliation problem in the spectral domain now becomes a least square problem with linear constraints. It reads:

$$\begin{aligned} \min \quad & f = (\widehat{Y} - Y_m)^T W^{-1} (\widehat{Y} - Y_m) \\ \text{s.t.} \quad & P\widehat{Y} = 0 \end{aligned} \qquad (15)$$

We hereby use the method suggested by Heyen et al. [13] to solve the above data reconciliation problem. The constrained optimization problem is transformed into a corresponding unconstrained problem [6], using the Lagrange multiplier vector v. The Lagrangian of the problem reads:

$$L(\widehat{Y}, v) = (\widehat{Y} - Y_m)^T W^{-1} (\widehat{Y} - Y_m) + 2v^T P\widehat{Y} \qquad (16)$$

In order to obtain the unknown variables, take partial derivatives and set them to zero:

$$\frac{\partial L}{\partial \widehat{Y}} = 2(\widehat{Y} - Y_m)^T W^{-1} + 2v^T P = 0$$

$$\frac{\partial L}{\partial v} = 2P\widehat{Y} = 0$$

(17)

Rewrite the above equations as

$$\begin{pmatrix} W^{-1} & P^T \\ P & \mathbf{0}_{\dim(v)\times\dim(v)} \end{pmatrix} \begin{pmatrix} \widehat{Y} \\ v \end{pmatrix} = \begin{pmatrix} W^{-1}Y_m \\ \mathbf{0}_{\dim(v)\times 1} \end{pmatrix}$$

(18)

Thus,

$$\widehat{Y} = \begin{pmatrix} \mathbf{I}_{\dim(Y_m)} & \mathbf{0}_{\dim(Y_m)\times\dim(v)} \end{pmatrix} \begin{pmatrix} W^{-1} & P^T \\ P & \mathbf{0}_{\dim(v)\times\dim(v)} \end{pmatrix}^{-1} \begin{pmatrix} W^{-1}Y_m \\ \mathbf{0}_{\dim(v)\times 1} \end{pmatrix}$$

(19)

where matrices $\mathbf{I}$ and $\mathbf{0}$ are Identity Matrix and Zero Matrix of appropriate size. Note that this problem can be solved numerically easily, with standard optimization software such as CPLEX, MATLAB and CVX [6].

The reconciliated measurements $\widehat{Y}$, can then be used to obtain the desired internal boundary conditions using Eqs. (10)–(12).

Remark 1. The proposed approach thus consists in assuming high confidence in the model, and finding the "best" estimation, i.e. the estimation which minimizes measurement error. This is a standard procedure in data reconciliation.

3. Application to the Sacramento River

3.1. Description of the system and assumption

The Sacramento-San Joaquin Delta in California is a valuable resource and an integral part of California's water system. This complex network covers 738,000 acres interlaced with over 1150 km of tidally influenced channels and sloughs. This network is monitored by a static sensor infrastructure subject to usual problems of inaccuracy and measurement errors for interested sensing systems. The area of interest for our experiment is located around the junction of the Sacramento River and the Georgiana Slough, as shown in Fig. 2. Most of the time, the direction of mean river flow is from north to south, as indicated with arrows. During the tidal inversion, the water flows in the opposite way. For experimental purposes, we need the boundary conditions at the three locations labeled A–C, but only get the measurements at SDC, DLC, GSS and GES. The method described in the previous section enables us to do that.

Four USGS stations, named SDC, DLC, GES and GSS, are located at the external boundaries of this deployment field. The stations are marked as squares in Fig. 2. Both discharge and stage are collected every 900 s at these stations. Note that in the USGS measurement system, only the stage are measured directly, the discharge data is estimated by a rating curve, which is a relation between stream stage and streamflow. The relation of stream stage to streamflow is always changing, and need to be calibrated frequently. It will introduce errors if the rating curve has not been validated in time. More detailed information can be found at http://ga.water.usgs.gov/edu/measureflow.html.

The field data was collected between 10/23/2007 and 11/13/2007. The raw field data is noisy, and the measurement errors are assumed to follow a normal Gaussian distribution. In addition, the following simplifications for the flow model have been made in this study:

- The flow can be represented by a one-dimensional model.
- The channel geometry is fixed, as the effects of sediment deposition and scour are negligible during the experiment period.
- The channel geometry can be modeled by a rectangular cross-section.
- The lateral and vertical accelerations are negligible.
- The pressure distribution is hydrostatic.
- There is no significant jump along the bathymetry of the channel, and the bed slope is smooth and small.
- The water surface across any cross-section is horizontal.

These assumptions have been verified in practice during experimental field deployments performed by our lab. The model parameters are the average free surface width T_{0i}, the average bottom slope S_{bi}, the average Manning's coefficient n, the average discharge Q_i, and the average downstream stage Y_{Xi} for each channel i ($i = 1, \ldots, 5$). These parameters are known to us experimentally. Based on measurements available to us at the SDC, DLC, GSS and GES, the field data at three intermediate locations in the channel network are chosen to assess the accuracy of the method (at locations marked in triangles).

3.2. Modal decomposition of the measured data

Since both the discharge and stage are measured at the four USGS stations (SDC, DLC, GSS and GES), the measured flow variable vector $Y_m(t)$ is
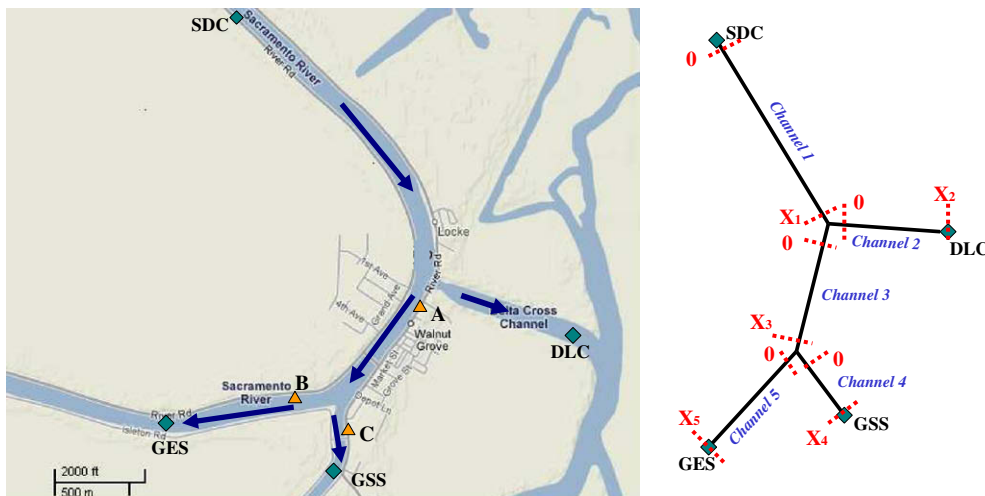

Fig. 2. Test area in the Sacramento River and the Georgiana Slough.

$$Y_m(t) = [q_1^m(0,t), y_1^m(0,t), q_2^m(X_2,t), y_2^m(X_2,t), q_4^m(X_4,t),$$
$$y_4^m(X_4,t), q_5^m(X_5,t), y_5^m(X_5,t)]^T \qquad (20)$$

where m stands for measured. The fundamental idea is to decompose the measured variables Y_m into a finite sum of N dominant oscillatory modes. In the case of a channel network influenced by the ocean at the downstream end, these modes are essentially the dominant modes produced by tidal forcing. The measured variables are therefore expressed using modal decomposition:

$$Y_m(t) = \sum_{k=0}^{N} [D_k e^{j\omega_k t} + \overline{D_k} e^{-j\omega_k t}] \qquad (21)$$

where

$$D_k = \left[d_k^{(1,1,0)}, d_k^{(1,2,0)}, d_k^{(2,1,X_2)}, d_k^{(2,2,X_2)}, d_k^{(4,1,X_4)}, d_k^{(4,2,X_4)}, d_k^{(5,1,X_5)}, d_k^{(5,2,X_5)} \right]^T \qquad (22)$$

$D_k = [d_k^{(\alpha,\beta,\gamma)}]^T$ are the Fourier coefficients of the spectral decomposition of Y_m, where α, β, γ represent the channel number, discharge/stage variable, location of each channel reach, respectively. ω_k's are the set of frequencies used for modal decomposition.

Fig. 3 shows the spectral analysis for the discharge data at station SDC: There are three dominant tidal frequencies in the system: $\omega_1 = 2.31 \times 10^{-5}$ s^{-1} (or period 12.4 h tide, corresponding to the M2 tide generated by the moon), $\omega_2 = 1.16 \times 10^{-5}$ s^{-1} (or period 24 h tide, corresponding to the K1 tide generated by the sun) and a $\omega_3 = 1.11 \times 10^{-5}$ s^{-1} (or period 25 h tide). The power spectrum is cut-off at 70 ft^3/s^2 to determine the 30 dominant frequencies. The second plot in Figs. 3 and 4 indicates that 30 modes are sufficient to capture the signal. The amplitude at 0 Hz is essentially the nominal stage. Similar arguments hold for the other measurements.

3.3. Hydraulic model of Sacramento River and Georgiana Slough

The open-channel network system in this study consists of five individual channels, as shown in Fig. 2. For each channel, the discharge and stage at upstream and downstream are related by a non-uniform transfer matrix:
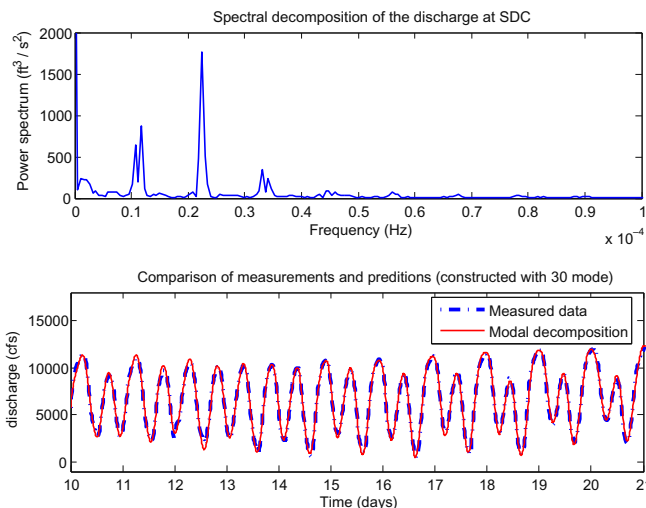

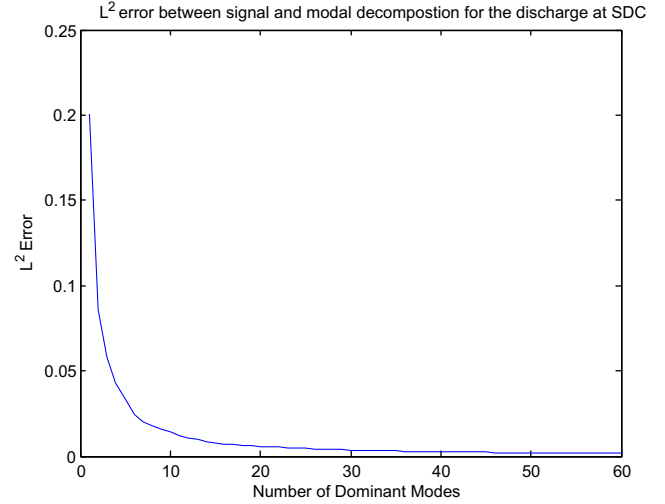**Fig. 3.** Spectral analysis of the discharge at the SDC station.

Fig. 4. Relative percent error between measurement data and modal representations as a function of the number of modes chosen for the decomposition.

$$\begin{pmatrix} q_i(X_i,s) \\ y_i(0,s) \end{pmatrix} = \begin{pmatrix} g_{i,11}^n(X_i,X_i,s) & g_{i,12}^n(X_i,X_i,s) \\ g_{i,21}^n(0,X_i,s) & g_{i,22}^n(0,X_i,s) \end{pmatrix} \begin{pmatrix} q_i(0,s) \\ y_i(X_i,s) \end{pmatrix},$$
$$i = 1,\dots,5 \qquad (23)$$

The linear relationships between internal boundary conditions at the two junctions are:

$$\begin{aligned}
&y_1(X_1,s) = y_2(0,s) \\
&y_2(0,s) = y_3(0,s) \\
&q_1(X_1,s) = q_2(0,s) + q_3(0,s) \\
&y_3(X_3,s) = y_4(0,s) \\
&y_4(0,s) = y_5(0,s) \\
&q_3(X_3,s) = q_4(0,s) + q_5(0,s)
\end{aligned} \qquad (24)$$

A total of 20 flow variables $q_i(x,s)$, $y_i(x,s)$ (for $x = 0$ or X_i, $i = 1,2,\dots,5$) are included in the system (23) and (24). These flow variables are related in a linear model $M(s)Z(s) = 0$ Eq. (10), with

$$Z(s) = [q_1(0,s), y_1(0,s), q_1(X_1,s), y_1(X_1,s), q_2(0,s),$$
$$y_2(0,s), q_2(X_2,s), y_2(X_2,s), q_3(0,s), y_3(0,s), q_3(X_3,s),$$
$$y_3(X_3,s), q_4(0,s), y_4(0,s), q_4(X_4,s), y_4(X_4,s), q_5(0,s),$$
$$y_5(0,s), q_5(X_5,s), y_5(X_5,s)]^T$$

Here, $M(s)$ is a 16 by 20 matrix, which encodes the 16 equations comprised of (23) (five channels), and (24) (internal boundary conditions).

Since rank$(M(s)) = 16$, given four boundary flow variables $Z_{given\,BC} \subset Z$, all the other sixteen boundary flow variables $Z_{other\,BC} = Z \setminus Z_{given\,BC}$ can be uniquely determined by the 16 equations set (23) and (24).

Let us assume that the four known external boundary conditions of the network are: the discharge at SDC: $q_1(0,s)$, the stage at DLC: $y_2(X_2,s)$, the stage at GSS: $y_4(X_4,s)$ and the stage at GES: $y_5(X_5,s)$. All the other boundary flow variables can be solved by Eq. (11). More specifically,

$$Z_{given\,BC} = [q_1(0,s), y_2(X_2,s), y_4(X_4,s), y_5(X_5,s)]^T$$

$$Z_{other\,BC} = [y_1(0,s), q_1(X_1,s), y_1(X_1,s), q_2(0,s), y_2(0,s),$$
$$q_2(X_2,s), q_3(0,s), y_3(0,s), q_3(X_3,s), y_3(X_3,s), q_4(0,s),$$
$$y_4(0,s), q_4(X_4,s), q_5(0,s), y_5(0,s), q_5(X_5,s)]^T$$

$$R(s) = R_1(s)^{-1} R_2(s)^T$$

$$
R_1(s) = \begin{pmatrix}
0 & 1 & -g_{1,12}(s) & 0 & 0 & 0 & 0 & 0 & 0 & 0 & 0 & 0 & 0 & 0 & 0 & 0 \\
1 & 0 & -g_{1,22}(s) & 0 & 0 & 0 & 0 & 0 & 0 & 0 & 0 & 0 & 0 & 0 & 0 & 0 \\
0 & 0 & 0 & -g_{2,11}(s) & 0 & 1 & 0 & 0 & 0 & 0 & 0 & 0 & 0 & 0 & 0 & 0 \\
0 & 0 & 0 & -g_{2,21}(s) & 1 & 0 & 0 & 0 & 0 & 0 & 0 & 0 & 0 & 0 & 0 & 0 \\
0 & 0 & 0 & 0 & 0 & 0 & g_{3,11}(s) & 0 & -1 & g_{3,12}(s) & 0 & 0 & 0 & 0 & 0 & 0 \\
0 & 0 & 0 & 0 & 0 & 0 & g_{3,21}(s) & 0 & -1 & g_{3,22}(s) & 0 & 0 & 0 & 0 & 0 & 0 \\
0 & 0 & 0 & 0 & 0 & 0 & 0 & 0 & 0 & 0 & -g_{4,11}(s) & 0 & 1 & 0 & 0 & 0 \\
0 & 0 & 0 & 0 & 0 & 0 & 0 & 0 & 0 & 0 & -g_{4,21}(s) & 1 & 0 & 0 & 0 & 0 \\
0 & 0 & 0 & 0 & 0 & 0 & 0 & 0 & 0 & 0 & 0 & 0 & -g_{5,11}(s) & 0 & 1 & 0 \\
0 & 0 & 0 & 0 & 0 & 0 & 0 & 0 & 0 & 0 & 0 & 0 & -g_{5,21}(s) & 1 & 0 & 0 \\
0 & 0 & 1 & 0 & -1 & 0 & 0 & 0 & 0 & 0 & 0 & 0 & 0 & 0 & 0 & 0 \\
0 & 0 & 1 & 0 & 0 & 0 & -1 & 0 & 0 & 0 & 0 & 0 & 0 & 0 & 0 & 0 \\
0 & -1 & 0 & 1 & 0 & 1 & 0 & 0 & 0 & 0 & 0 & 0 & 0 & 0 & 0 & 0 \\
0 & 0 & 0 & 0 & 0 & 0 & 0 & 0 & 0 & 1 & 0 & -1 & 0 & 0 & 0 & 0 \\
0 & 0 & 0 & 0 & 0 & 0 & 0 & 0 & 0 & 1 & 0 & 0 & 0 & 0 & -1 & 0 \\
0 & 0 & 0 & 0 & 0 & 0 & 0 & 0 & 1 & 0 & -1 & 0 & 0 & -1 & 0 & 0
\end{pmatrix}
$$

$$
R_2(s) = \begin{pmatrix}
g_{1,11}(s) & g_{1,21}(s) & 0 & 0 & 0 & 0 & 0 & 0 & 0 & 0 & 0 & 0 & 0 & 0 & 0 & 0 \\
0 & 0 & g_{2,12}(s) & g_{2,22}(s) & 0 & 0 & 0 & 0 & 0 & 0 & 0 & 0 & 0 & 0 & 0 & 0 \\
0 & 0 & 0 & 0 & 0 & 0 & g_{4,12}(s) & g_{4,22}(s) & 0 & 0 & 0 & 0 & 0 & 0 & 0 & 0 \\
0 & 0 & 0 & 0 & 0 & 0 & 0 & 0 & g_{5,12}(s) & g_{5,22}(s) & 0 & 0 & 0 & 0 & 0 & 0
\end{pmatrix}
$$

The parameters of the model are listed in Table 1. The mean discharge (Q_{0i}) of the channels 1, 2, 4, 5 are computed using the measured discharge at SDC, DLC, GSS, GES, respectively. It is clear that the measurement data are inconsistent, since $Q_{01} \neq Q_{02} + Q_{04} + Q_{05}$. To partially compensate for the measurement error, the mean discharge at channel 3 is set to be: $Q_{03} = [(Q_{01} - Q_{02}) + (Q_{04} + Q_{05})]/2$.

3.4. Data reconciliation

Let us assume that the measured variables Y_m are independent and subject to a Gaussian distributed noise. Based on the static model (11), the measurable variables are linked by a static relationship of the following form:

$$P(s)Y(s) = 0 \tag{25}$$

where

$$
P(s) = \begin{bmatrix}
R(s)_{1,1} & R(s)_{1,2} & R(s)_{1,3} & R(s)_{1,4} & -1 & 0 & 0 & 0 \\
R(s)_{6,1} & R(s)_{6,2} & R(s)_{6,3} & R(s)_{6,4} & 0 & -1 & 0 & 0 \\
R(s)_{13,1} & R(s)_{13,2} & R(s)_{13,3} & R(s)_{13,4} & 0 & 0 & -1 & 0 \\
R(s)_{16,1} & R(s)_{16,2} & R(s)_{16,3} & R(s)_{16,4} & 0 & 0 & 0 & -1
\end{bmatrix}
$$

given $Y(s) \setminus Z_{given\,BC}$ is the first, sixth, thirteenth and sixteenth element of $Z_{other\,BC}$. Now, combining the solution of the data reconciliation problem (19) with the static model (25), reconciliated measurements $\widehat{Y}$ can be calculated. Assume that $\widehat{Y}$ is in the form:

$$\widehat{Y}(t) = \sum_{k=0}^{N}[B_k e^{j\omega_k t} + \overline{B_k} e^{-j\omega_k t}] \tag{26}$$

where $B_k = [b_k^{(\alpha,\beta,\gamma)}]^T$ is the Fourier coefficients vector of the spectral decomposition of $\widehat{Y}$, and α, β, γ represent the channel number, discharge/stage variable, location of each channel reach, respectively,

$$B_k = [b_k^{(1,1,0)}, b_k^{(1,2,0)}, b_k^{(2,1,X_2)}, b_k^{(2,2,X_2)}, b_k^{(4,1,X_4)}, b_k^{(4,2,X_4)}, b_k^{(5,1,X_5)}, b_k^{(5,2,X_5)}]^T \tag{27}$$

For specific dominant ω_k, $k = 1, \ldots, N$, the coefficient vector B_k in Eq. (26) is calculated by Eq. (19):

$$B_k = (\mathbf{I}_{8,8} \quad \mathbf{0}_{8,4}) \begin{pmatrix} W^{-1} & P(s)^T \\ P(s) & \mathbf{0}_{4,4} \end{pmatrix}^{-1} \begin{pmatrix} W^{-1}D_k \\ \mathbf{0}_{4,1} \end{pmatrix} \tag{28}$$

The reconciliated boundary condition data is shown and compared to measured data in Figs. 5 and 6. For clarity, the mean flow has been subtracted from the plots in the interest of magnifying the display scale. From the figures, the reconciliated data is very close to

Table 1
Parameters for the Sacramento River and the Georgiana Slough.

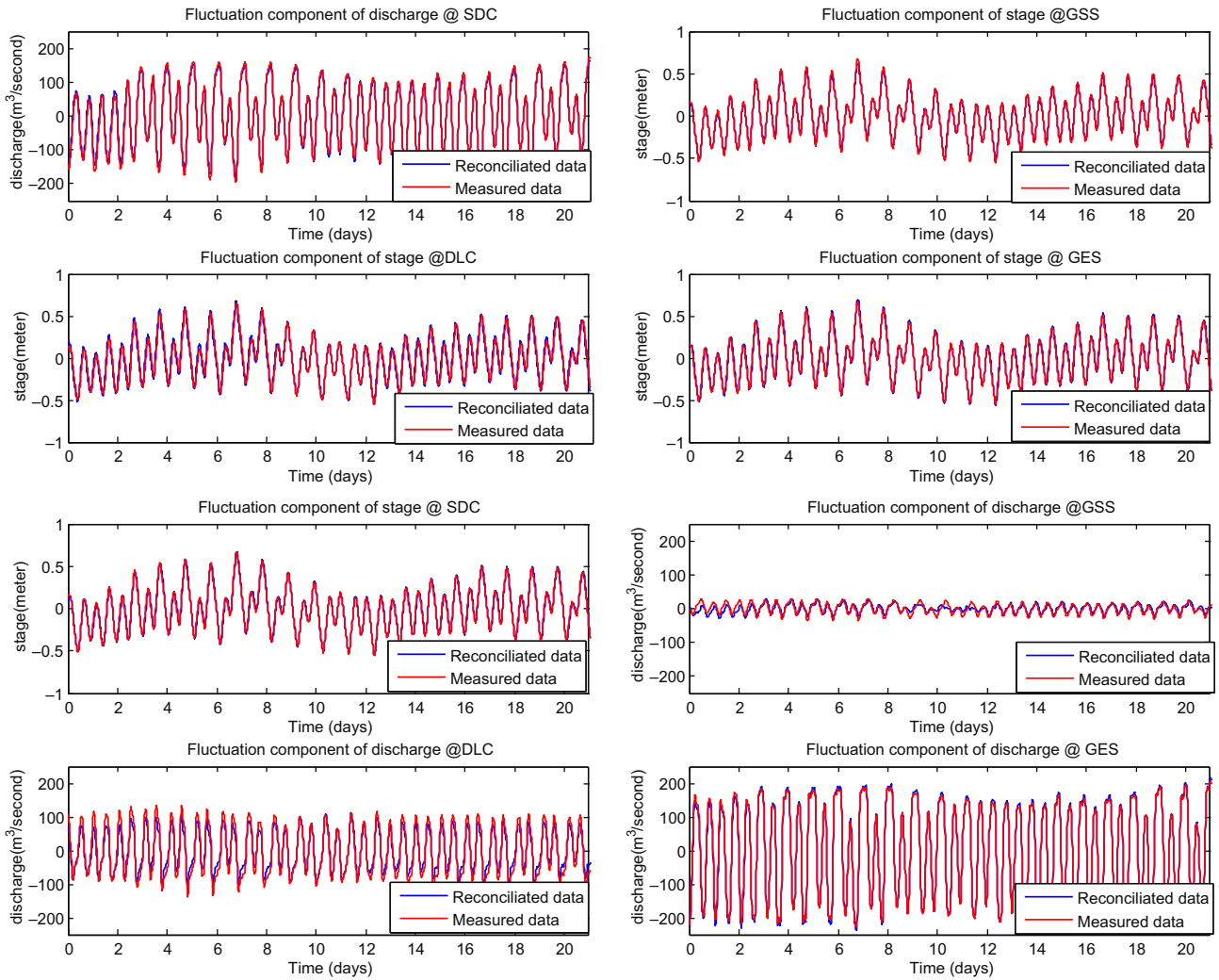| Channel	Q_{0i} (m^3 s^{-1})	Y_{Xi} (m)	T_{0i} (m)	S_{bi} (m/km)	n (m$^{-1/3}$ s)	X_i (m)	C_0 (m/s)	X_i/C_0 (s)
$i = 1$	186.7	5.6	115	−0.04	0.0323	2800	7.42	377.4
$i = 2$	83.9	4.1	110	−0.09	0.0323	2000	6.30	317.5
$i = 3$	113.1	7.7	110	−0.04	0.0323	1300	8.71	149.3
$i = 4$	58.1	4.0	56	−0.19	0.0323	600	3.40	176.5
$i = 5$	65.2	5.3	89	−0.04	0.0323	1600	7.19	222.5

Fig. 5. Reconciliated boundary condition data vs. measured data.

the measurements. The difference between the reconciliated data and measurements is further evaluated in Table 2. Three primary evaluation measures are analyzed here:

- The maximum value is the maximum difference between the reconciliated and measured data at the same time steps.
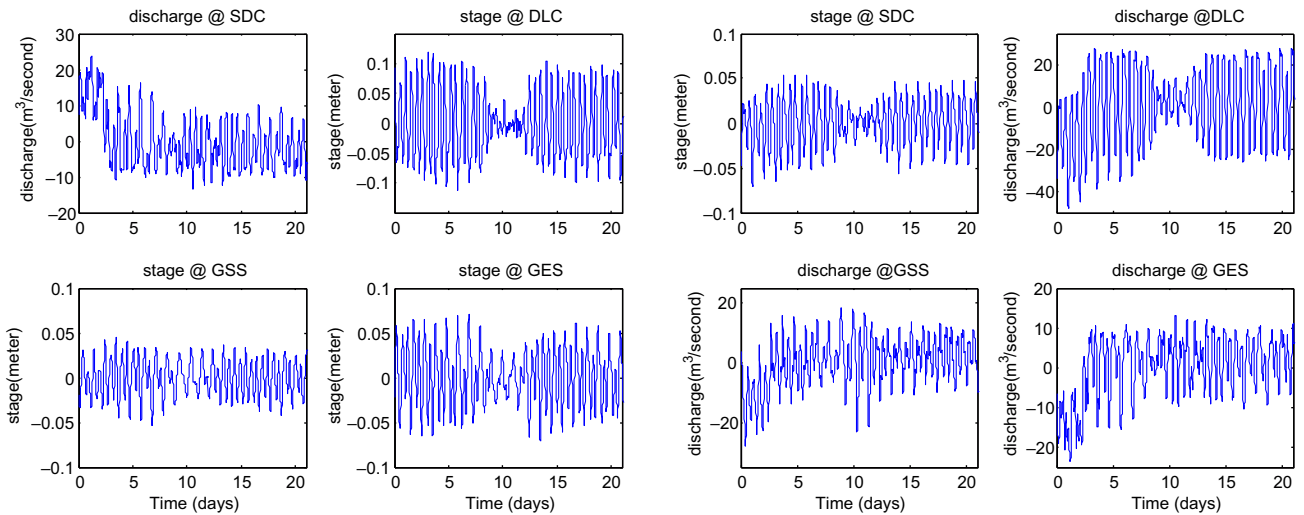- The coefficient of efficiency E is defined as [18]:

Fig. 6. The difference between reconciliated data and measured data.

Table 2
Max-value, ρ-value and E-value for reconciliated data and measured data.

Variable	USGS station	Max-value	E-value	ρ-value
Discharge	SDC	23.66 m³/s	0.9930	0.9975
	DLC	28.23 m³/s	0.9368	0.9883
	GES	13.00 m³/s	0.9968	0.9985
	GSS	18.41 m³/s	0.9368	0.8369
Stage	SDC	0.05 m	0.9889	0.9947
	DLC	0.12 m	0.9504	0.9759
	GES	0.07 m	0.9847	0.9935
	GSS	0.05 m	0.9938	0.9989

$$E = 1 - \left[\frac{\sum_{i=1}^{N}(\hat{u}_i - u_i)^2}{\sum_{i=1}^{N}(u_i - \overline{u_i})^2} \right] \quad (29)$$

where u_i is the flow variable of interest (for example q_i or y_i in this study), $\hat{u}_i$ is the reconciliated/modeled flow variable, $\overline{u_i}$ is the mean of u_i, for $i = 1, 2, \ldots, N$ measurement events. If the measured data is perfect, $E = 1$. If $E < 0$, the corresponding measurement is not reasonable and must be excluded from the modeling procedure.

- The last statistic evaluation of the analysis is the correlation coefficient ρ, given by

$$\rho = \frac{\sum_1^N (u_i - \overline{u_i})(\hat{u}_i - \overline{\hat{u}_i})}{\sqrt{\sum_1^N (u_i - \overline{u_i})^2 \sum_1^N (\hat{u}_i - \overline{\hat{u}_i})^2}} \quad (30)$$

where $\overline{\hat{u}_i}$ represents the mean of reconciliated flow for $i = 1, 2, \ldots, N$ measurement events.

3.5. Method validation

We used existing USGS sensors in place in the Delta as measurement points, and deploy our own sensors at selected locations to produce data used for the validation. We validate the method by using existing and deployable monitoring infrastructure: USGS fixed sensor stations (see Fig. 7) are used as measurement points (see exact location in Fig. 2); deployable UC Berkeley sensors (see Fig. 7) are placed at locations A–C on the map of Fig. 2. The measurements were collected between 11/01/2007 and 11/12/2007, and serve as a validation data set for this method.

Location A is downstream of the junction of Sacramento River and Delta Cross channel; Location B is downstream of GSS branch; Location C is downstream of Sacramento Branch. Without loss of

Fig. 7. (Left) USGS sensor station at *GSS*, used as a measurement sensor. (Right) Deployable ADCP sensor, used in Section 3.5 for gathering the validation data (three of them were deployed between 11/01/2007 and 11/12/2007 in order to gather the data for this study).

generality, the discharge at Location A, along with the stage data at three locations, are used to test the model.

### 3.5.1. Model validation with measured boundary conditions

Following the steps described in Section 2, the flow variables at the boundaries of each branch $Z_{other\,BC}$ are calculated using Eq. (11). Here, the measured discharge at SDC, stage at DLC, GES, GSS are used as $Z_{given\,BC}$. The flow variables along each branch are estimated using the non-uniform transfer matrix (Eq. (12)). The simulation results are shown in Fig. 8.

Model calibration and validation are further evaluated using E-value and ρ-value. Table 3 summarizes the values of ρ and E in the validation sets of our channel flow model.

From Fig. 8 and Table 3, it is clear that Location A is the location where the discharge is estimated with the least precision, as the

Table 3
ρ-Value and E-value for model validation without reconciliation (Section 3.5.1).

Location	A	A	B	C
Variables	Discharge	Stage	Stage	Stage
E	0.7219	0.9820	0.9796	0.9807
ρ	0.8555	0.9922	0.9916	0.9927
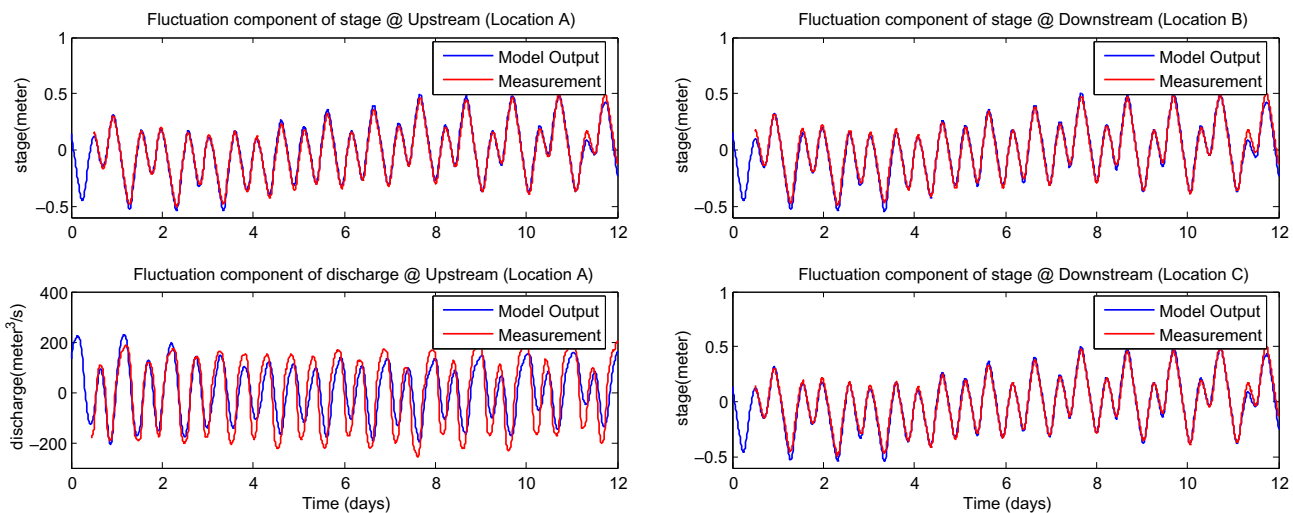
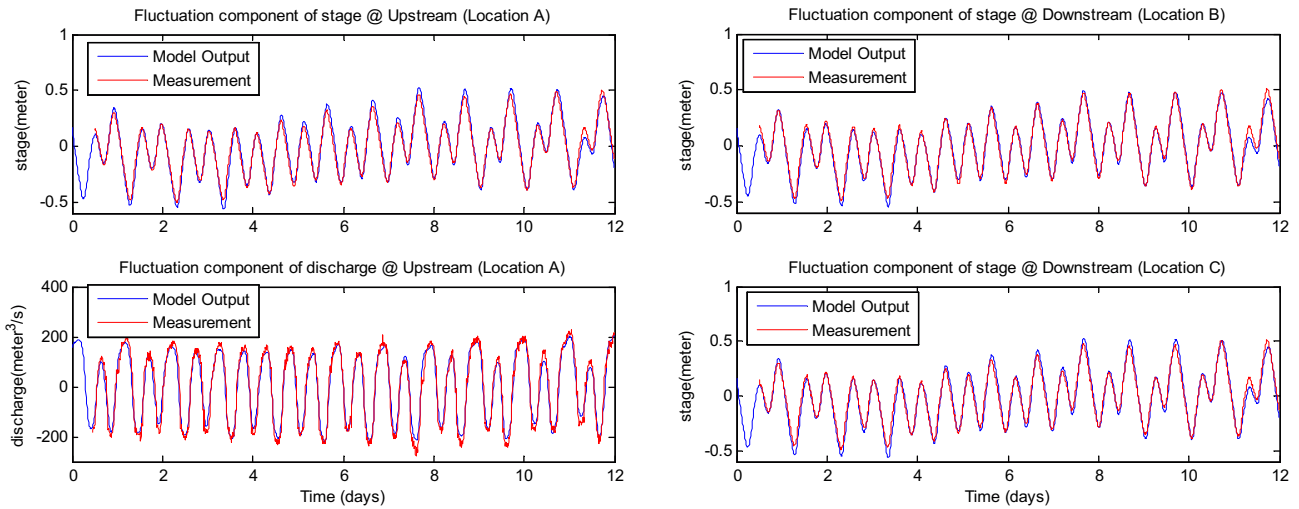**Fig. 8.** Validation of the model output with measurement using USGS measurements.

Fig. 9. Validation of the model output with measurement using reconciliated BC.

characteristics of either the phase or the amplitude suffer a significant offset. Although we have a precise stage estimation at Locations A–C, the model does not provide enough information to characterize the flow in the experiment area.

3.5.2. Modal validation with reconciliated boundary conditions based on all the measurements

We will use reconciliated data shown in Fig. 5 as $Z_{given\,BC}$. The flow variables $Z_{other\,BC}$, $q_i(s,x)$, $y_i(x,s)$ are calculated using Eqs. (11) and (12). The simulation results are shown in Fig. 9.

The values of ρ and E are listed in Table 4. Both ρ-values and E-values are close to unity. Table 4 and Fig. 9 thus indicate that the proposed model reconciliation approach provides a higher accuracy in the flow estimation.

Table 4
ρ-Value and E-value for model validation after reconciliation (Section 3.5.2).

Location	A	A	B	C
Variables	Discharge	Stage	Stage	Stage
E	0.9775	0.9643	0.9768	0.9612
ρ	0.9895	0.9876	0.9897	0.9875

3.5.3. Exclusion of erroneous sensors

The data reconciliation method enables us to detect and exclude sensors with erroneous measurements and further assess the boundary conditions using the remaining properly working sensors. Based on known results in data reconciliation, when the reconciliated data is close to the "true" data, the difference between the reconciliated and measured data must follow a Gaussian distribution with a zero mean. If this condition is not satisfied, the sensor is deemed to be malfunctioning and not suitable for measurements.

In order to test the performance of our method, we first intentionally add a large (10 times in magnitude) perturbation to the discharge data measured at DLC, and conduct the standard data reconciliation procedure described in preceding sections. The probability density function of the difference between the reconciliated data and measured data $(\hat{Y} - Y_m)$ is calculated and compared in Fig. 10. A Pearson's chi-square (χ^2) test is further applied to assess whether this probability distribution differs from a theoretical Gaussian distribution [19,3]. The Pearson's χ^2 statistic is calculated as

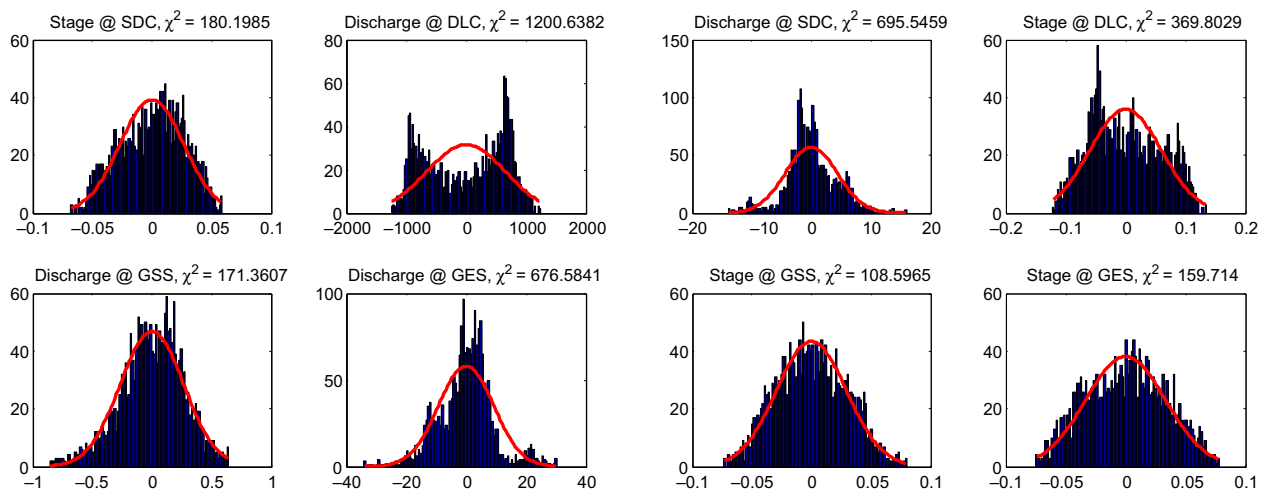$$\chi^2 = \sum_{i=1}^{n} \frac{(O_i - E_i)^2}{E_i} \tag{31}$$

Fig. 10. Error distribution between the reconciliated data and USGS measurements (perturbation discharge at DLC is added on purpose in the data set).
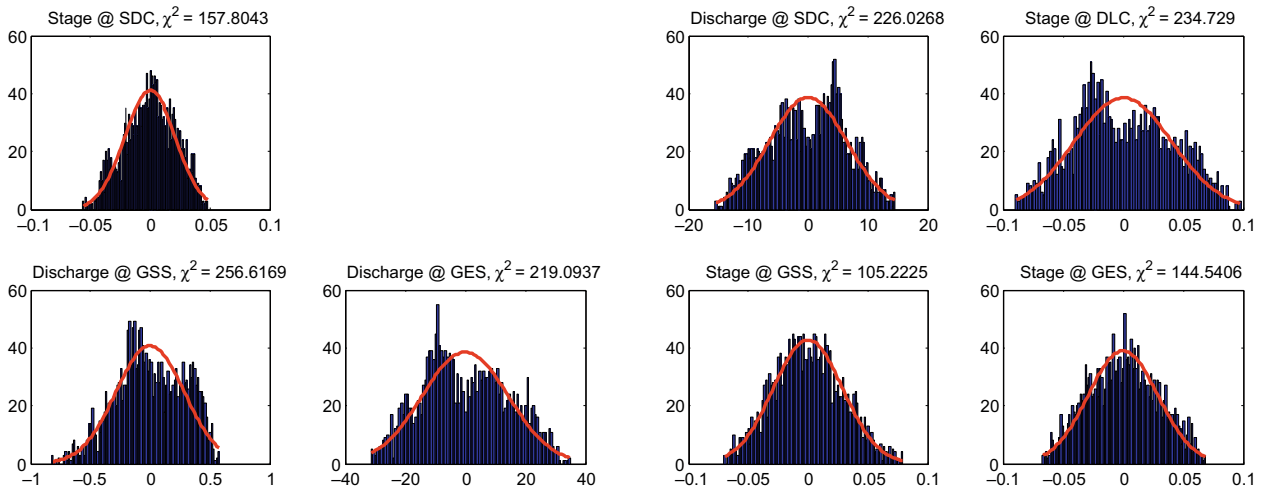
Fig. 11. Error distribution between reconciliated and measured data (discharge at DLC is removed from the data reconciliation process).

where χ^2 is the test statistic that asymptotically approaches a χ^2 distribution; O_i an observed frequency; E_i a theoretical (Gaussian) frequency; n is the number of possible outcomes of each event.

From the data (see in particular subfigure in Fig. 10), it is obvious that the difference between the measured and reconciliated discharge at station DLC does not follow the Gaussian distribution, implying that the sensor is malfunctioning and should be excluded from the data sets.

We then remove the discharge at DLC from the measurement data, and repeat the data reconciliation procedure. The probability density functions are showed in Fig. 11. The difference between the reconciliated data and USGS measurements is then more likely to follow a standard Gaussian distribution.

In summary, the χ^2 values are evaluated and assembled in Table 5. Note that a small χ^2-value indicates that the observation data distribution is likely to follow a normal distribution.

Furthermore, we use the same three locations (A–C) in the experiment domain to validate the reconciliated data. Table 6 compares the ρ-value and E-value for the two cases: with the erroneous sensor and without the erroneous sensor.

It is rather interesting to note that modal output is not affected by the intentionally perturbed sensor data, meaning that the data reconciliation method is robust enough to provide satisfactory boundary conditions even if one of the sensors is malfunctioning.

4. Conclusions

This article proposes a new method to estimate the flow variables in a channel network system subject to periodic forcing. A spatially dependent channel network model is constructed in the frequency domain using LSWE transfer matrix for the non-uniform steady state case. Modal decomposition allows the output response to be expressed in terms of the spectral coefficients of the input variables and the transfer matrix coefficients evaluated at appropriate locations. Data reconciliation in this case is reduced to a static least-square minimization problem in the frequency domain, and enables an efficient reconstruction of noisy boundary measurements. Subsequently, the flow properties at any location in the system can be readily predicted. The approach proposed in this study has been applied to a channel network in the Sacramento-San Joaquin Delta, using four USGS fixed sensors as measurement points. The flow prediction was successfully validated at three intermediate locations of the channel system, using deployed sensors from UC Berkeley.

This method is now used for short-term forecast of internal condition in the Georgiana Slough and Sacramento River, which we use for our experimental drifter and submarine deployments. This information is particularly useful for our ongoing data assimilation and inverse modeling studies currently underway, using Lagrangian sensors.

Table 5
χ^2 value for different cases.

Variables	With wrong DLC discharge data	Without DLC discharge data
Discharge at SDC	695.55	157.80
Stage at SDC	180.20	226.03
Discharge at DLC	1200.64	N/A
Stage at DLC	369.80	234.73
Discharge at GSS	171.36	256.62
Stage at GSS	106.60	105.22
Discharge at GES	675.58	219.09
Stage at GES	159.71	144.54

Table 6
ρ-Value and E-value for modal validation (with and without discharge at DLC).

Location	A	A	B	C
Variables	Discharge	Stage	Stage	Stage
E (with wrong sensor)	0.9777	0.9599	0.9762	0.9567
E (without wrong sensor)	0.9676	0.9651	0.9788	0.9611
ρ (with wrong sensor)	0.9889	0.9867	0.9894	0.9867
ρ (without wrong sensor)	0.9893	0.9892	0.9908	0.9891

Appendix A. Transfer matrix representation of linearized Saint-Venant model

The application of Laplace transform to the linear PDE system (6) leads to the *ordinary differential equations* (ODEs) in the variable x, with a complex parameter s

$$\begin{pmatrix} q(x,s) \\ y(x,s) \end{pmatrix}_x = \mathscr{G}_s(x) \begin{pmatrix} q(x,s) \\ y(x,s) \end{pmatrix} \tag{A.1}$$

In the case of designing and analyzing small-scale flood management systems, such as storm sewers and highway drainage, *Uniform Flow* is a good simplified model which assume the channel invert slope and the energy grade line slope are equal ($S_b = S_f$). However, in real-world situation, this assumption is rarely represented, and backwater approximation is introduced to simulate the *Non-uniform Flow*.

• *Transfer matrix for uniform flow*

Remark 2 (*Uniform flow*). In the case of uniform flow, the flow variables are constant along the length of the channel, i.e., the discharge $Q_0(x) = Q_0 = Q_X$ and the stage $Y_0(x) = Y_n$ (normal depth).

A closed-form solution of the linearized Saint-Venant equations in the uniform flow case can be obtained, relating the flow variables at any point x of the river reach $q(x,s), y(x,s)$ to the boundary conditions $q(0,s)$ and $y(X,s)$ (referring to Litrico and Fromion [15] for details):

$$\begin{pmatrix} q(x,s) \\ y(x,s) \end{pmatrix} = \begin{pmatrix} g_{11}^u(x,X,s) & g_{12}^u(x,X,s) \\ g_{21}^u(x,X,s) & g_{22}^u(x,X,s) \end{pmatrix} \begin{pmatrix} q(0,s) \\ y(X,s) \end{pmatrix} \tag{A.2}$$

where

$$g_{11}^u(x,X,s) = \frac{\lambda_2 e^{\lambda_1 x + \lambda_2 X} - \lambda_1 e^{\lambda_2 x + \lambda_1 X}}{\lambda_2 e^{\lambda_2 X} - \lambda_1 e^{\lambda_1 X}}$$

$$g_{12}^u(x,X,s) = T_0 s \frac{e^{\lambda_1 x} - e^{\lambda_2 x}}{\lambda_2 e^{\lambda_2 X} - \lambda_1 e^{\lambda_1 X}}$$

$$g_{21}^u(x,X,s) = \frac{\lambda_1 \lambda_2}{T_0 s} \frac{e^{\lambda_2 X + \lambda_1 X} - e^{\lambda_1 x + \lambda_2 X}}{\lambda_2 e^{\lambda_2 X} - \lambda_1 e^{\lambda_1 X}}$$

$$g_{22}^u(x,X,s) = \frac{\lambda_2 e^{\lambda_2 x} - \lambda_1 e^{\lambda_1 x}}{\lambda_2 e^{\lambda_2 X} - \lambda_1 e^{\lambda_1 X}}$$

Here, λ_1 and λ_2 are the eigenvalues of the ODE system (A.1), and are given by

$$\lambda_i(s) = \frac{2T_0 V_0 s + \gamma_0}{2\alpha_0} + (-1)^i \frac{\sqrt{4C_0^2 T_0^2 s^2 + 4T_0(V_0\gamma_0 - \alpha_0\beta_0)s + \gamma_0^2}}{2\alpha_0} \tag{A.3}$$

In the following sections, the transfer matrix for the uniform case is denoted as $\mathscr{G}^u(x,X,s) = (g_{ij}^u(x,X,s))$.

• *Transfer matrix for non-uniform flow* To solve a hydraulic problem in realistic cases, the backwater approximation is assumed to study flow regimes, in which the water elevation is not constant along the reach [22]. Following the method in [22], and further modified in [16], the backwater curve defined by Eq. (A.5) is approximated by two straight lines, as shown in Fig. 12:

$$\frac{dQ_0(x)}{dx} = 0 \tag{A.4}$$

$$\frac{dY_0(x)}{dx} = \frac{S_b - S_{f0}}{1 - F_0(x)^2} \tag{A.5}$$

The river reach is then decomposed into two parts: a uniform part and a backwater part. The intersection of the two parts is
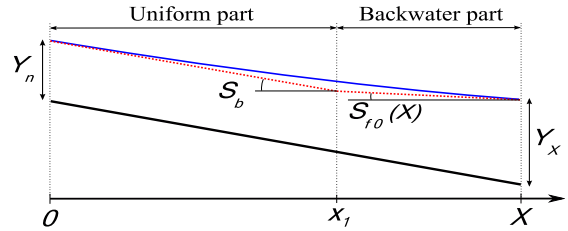

Fig. 12. Backwater curve approximation.

denoted by x_1. Let x_u denote the location in the uniform part, $x_b = x - x_1$ denote the location in the backwater part, $X_u = x_1$ denote the length of the uniform part, and $X_b = X - x_1$ denote the length of the backwater part. Let $\mathscr{G}^u(x_u, X_u, s)$ and $\mathscr{G}^b(x_b, X_b, s)$ denote the transfer matrices for the uniform and backwater parts, respectively; while $\mathscr{G}^b(x_b, X_b, s)$ has the same form as the transfer matrix $\mathscr{G}^u(x_u, X_u, s)$. The transfer matrix for the non-uniform channel $\mathscr{G}^n(x, X, s) = (g_{ij}^n(x, X, s))$ compromises $\mathscr{G}^u(x_u, X_u, s)$ and $\mathscr{G}^b(x_b, X_b, s)$ with:

$$\begin{pmatrix} q(x,s) \\ y(x,s) \end{pmatrix} = \begin{pmatrix} g_{11}^n(x,X,s) & g_{12}^n(x,X,s) \\ g_{21}^n(x,X,s) & g_{22}^n(x,X,s) \end{pmatrix} \begin{pmatrix} q(0,s) \\ y(X,s) \end{pmatrix} \tag{A.6}$$

The detail of entries of the transfer matrix for the non-uniform case $\mathscr{G}^n(x, X, s) = (g_{ij}^n(x, X, s))$ is listed in [24].

References

[1] Albuquerque JS, Biegler LT. Data reconciliation and gross-error detection for dynamic systems. Am Inst Chem Eng J 1996;42(10):2481–586.
[2] Alhaj-Dibo M, Maquin D, Ragot J. Data reconciliation: a robust approach using a contaminated distribution. Control Eng Pract 2008;16:159–70.
[3] Bagajewicz MJ, Cabrera E. Data reconciliation in gas pipeline systems. Ind Eng Chem Res 2003;42(22):5596–606.
[4] Baume JP, Sau J. Study of irrigation cannal dynamics for control purposes. In: Proceedings of the international workshop in regulation of irrigation canals, Marrakech, Morroco; 1997.
[5] Bedjaoui N, Litrico X, Koenig D, Ribot-Bruno J, Malaterre P-O. Static and dynamic data reconciliation for an irrigation canal. J Irrigat Drain Eng, in press.
[6] Boyd S, Vandenberghe L. Convex optimization. New York: Cambridge University Press; 2004.
[7] Chow V. Open-channel hydraulics. New York: McGraw-Hill Book Company; 1988.
[8] Chui CK, Chen G. Kalman filtering with real time applications. Berlin: Springer-Verlag; 1998.
[9] Corriga R, Patta FF, Sanna S, Usai G. A mathematical model for open channel networks. Appl Math Modell 1979;23:51–4.
[10] Crowe CM. Data reconciliation – progress and challenge. J Process Control 1996;6(2):89–98.
[11] Deltour J, Canivet E, Sanfilippo F, Sau J. Data reconciliation on the complex hydraulic system of canal de provence. J Irrig Drain Eng 2005;131(3):291–7.
[12] Ermolin Y. Study of open-channel dynamics as controlled process. J Hydraul Eng 1992;119(1):59–71.
[13] Heyen G, Dumont MN, Kalitventzeff B. Computer-aided design of redundant sensor networks. Comput Chem Eng 2002;10:685–90.
[14] Lee MT, Delleur JW. A variable source area model of the rainfall–runoff process based on the watershed stream network. Water Resour Res 1976;12(5):1029–36.
[15] Litrico X, Fromion V. Frequency modeling of open channel flow. J Hydraul Eng 2004;130(8):806–15.
[16] Litrico X, Fromion V. Simplified modeling of irrigation canals for controller design. J Irrig Drain Eng 2004;130(5):373–83.
[17] Litrico X, Fromion V. Boundary control of linearized Saint-Venant equations oscillating modes. Automatica 2006;42(6):967–72.
[18] Nash JE, Sutcliffe JV. River flow forecasting through conceptual models. Part I: A discussion of principles. J Hydrol 1970;10:282–90.
[19] Plackett RL. Karl pearson and the chi-squared test. Int Stat Rev 1983;51(1):59–72.
[20] Ragot J, Maquin D. Reformulation of data reconciliation problem with unknown-but-bounded errors. Ind Eng Chem Res 2004;43(6):1530–6.
[21] Reimers C, Werther J, Gruhn G. Flowsheet simulation of solids processes data reconciliation and adjustment of model parameters. Chem Eng Process 2008;47:138–58.

[22] Schuurmans J, Clemmens AJ, Dijkstra S, Hof A, Brouwer R. Modeling of irrigation and drainage canals for controller design. J Irrig Drain Eng 1999;125(6):338–44.

[23] Tossavainen O-P, Percelay J, Tinka A, Wu Q, Bayen A. Ensemble Kalman filter based state estimation in 2D shallow water equations using lagrangian sensing and state augmentation. In: Proceedings of the 46th conference of decision and control; 2008.

[24] Wu Q, Amin S, Munier S, Bayen A, Litrico X, Belaud G. Parameter identification for the shallow water equations using modal decomposition. In: Proceedings of the 46th conference of decision and control; 2007.

[25] Wu Q, Litrico X, Bayen A. Open channel flow estimation and data reconciliation using modal decomposition. In: Proceedings of the 46th conference of decision and control; 2008.